Available online at www.sciencedirect.com
ScienceDirect
Thin Solid Films 515 (2007) 6943–6948
www.elsevier.com/locate/tsf

Electroluminescence and electron transport characteristics of aromatic polyimides containing 1,3,4-oxadiazole moiety

Shou-Chian Hsu [a], Wha-Tzong Whang [a,*], Ching-Shiun Chao [b]

[a] Institute of Materials Science and Engineering, National Chiao Tung University, 1001 Ta Hsueh Road, Hsin Chu, Taiwan, ROC
[b] Department of Material Science and Engineering, MingDao University, 369 Wen-Hua Road, Peetow, Chang Hua 52345, Taiwan, ROC

Received 13 April 2006; received in revised form 4 January 2007; accepted 7 February 2007
Available online 16 February 2007

Abstract

Single and double layer polymer light-emitting diodes (LEDs) were fabricated by using 2,5-bis(4-aminophenyl)-1,3,4-oxadiazole (BAO)-based aromatic polyimides (APIs). All the resultant APIs have high glass transition temperatures (T_g>250 °C) and high thermal decomposition temperatures (T_d>510 °C). The APIs exhibit broad fluorescent characteristic, and the fluorescent intensity is related to the intermolecular chain's orientation. BAO-3,3′-oxydiphthalic anhydride (ODPA) and BAO-4,4′-(hexafluoro-*iso*-propylidene) diphthalic anhydride show electroluminescent property in single layer LED devices. By inserting BAO-ODPA in the poly(*p*-phenylene vinylene)–poly(vinylalcohol) LED device to form a double layer device, the EL efficiency can be improved by two orders of magnitude.

Keywords: Polyimides; Electroluminescence; Charge transfer

1. Introduction

Aromatic polyimides (APIs) have been widely used in aerospace and automotive industries, and as alignment layers for liquid crystal displays, interlayer dielectric insulators, in the microelectronics industry because of their low dielectric constants, low coefficient of thermal expansion, high glass transition, and high radiation resistance. These excellent physical properties result from rigid polymer structures and strong intermolecular interactions.

APIs are usually synthesized through a two-step method: preparation of poly(amic acids) (PAAs) and then thermal or chemical imidization. The PAA polymerization rates relate to the electron affinity (E_a) of dianhydrides as an electron-acceptor and the ionization potential of diamines as an electron-donor. This suggests that charge transfer (CT) interaction may occur between the electron-donor and electron-acceptor fragments of the APIs [1]. Many previous works had reported the relationship between CT and fluorescence in APIs [2–13]. Wachsman and Frank [2] observed a significant increase in the CT fluorescence intensity with increased molecular aggregation resulting from increased imidization temperature. H. Luo et al. [3] reported that an increased concentration of polyimide led to denser packing of the polymer chains then increasing the CT fluorescence. However, aggregation would be one of the main barriers to high luminescence quantum yield in the conjugated polymer [14,15]. This hints that APIs could develop a different fluorescence mechanism in comparison with conjugated polymers.

Polymer light-emitting diodes (PLEDs) have attracted much interest in display application due to their excellent mechanical properties, tunable emission and low fabrication cost. However, one of the serious problems of PLED is the poor durability under operation owing to the flexibility and crystallization, oxidation and photodegradation characteristics of the organic materials [16,17]. The glass transition temperature (T_g) of the polymer is an important property for the application of PLED, because an emission layer would be easily relaxed during operation by Joule heating and results in the device failure [18]. However, application of thermostable polymers in PLED can improve the lifetime of polymer-based devices. Some research groups have demonstrated significant improvements in

* Corresponding author. Tel.: +886 3 5731873; fax: +886 3 5724727.
E-mail address: wtwhang@cc.nctu.edu.tw (W.-T. Whang).

0040-6090/$ - see front matter © 2007 Elsevier B.V. All rights reserved.
doi:10.1016/j.tsf.2007.02.015

photoluminescence or electroluminescence (EL) by using polyimides as a hole transport material [19–24]. Polyimides which contain the moieties of anthracence, perylene, metal complex, tetraphenyl terabiphenyl-*p*-quinquephenyl, 2,5-distyrylpyrazine, dibenzofurane, and furyl-substituted biphenylene were used as light-emitting materials [25–36].

In this study, the thermo properties of the 2,5-bis(4-aminophenyl)-1,3,4-oxadiazole (BAO)-based APIs were obtained. We have then investigated the relationship between the different dianhydride structures and aggregation, and examined the influence of CT interactions on the fluorescence behavior. We further fabricated single and double layer API LED devices to understand the electron transport characteristics of the APIs and their influence on light-emitting characteristics.

2. Experimental section

2.1. Materials

2,5-Bis(4-aminophenyl)-1,3,4-oxadiazole (BAO, 98% purity) was purchased from Lancaster, and was prior dried in a vacuum oven at 120 °C for 3 h before use. 3,3′-Oxydiphthalic anhydride (ODPA, 98% purity) and pyromellitic dianhydride (PMDA, 98% purity) were purchased from Tokyo Chemical Industry. 4,4′-(Hexafluoro-*iso*-propylidene) diphthalic anhydride (6FDA) and 4,4′-(4,4′-isopropylidenediphenoxy)bis (phthalic anhydride) (BPADA) were purchased from Aldrich. All the dianhydrides were purified by recrystallization using acetic anhydride, and then dried in a vacuum oven at 125 °C for 12 h. *N*,*N*-Dimethylacetamide (DMAc) was purchased from Tedia Company, and was dehydrated by using molecular sieves.

2.2. Preparation of the API films

The synthetic route of the BAO-based APIs is shown in Scheme 1. In a typical procedure, BAO (1.00 mmol) was first dissolved in DMAc (4 ml) under nitrogen stream at room temperature, then the dianhydride (1.00 mmol) was added into the BAO solution by five portions. After the complete dissolution of dianhydride, the reaction was further stirred at room temperature for 3 h to form the PAA solution. The PAA solution (15 wt.%) was cast on a glass plate, and then step-heated at 100 °C, 150 °C, 200 °C, and 250 °C, each one for an hour to obtain the API films with thickness of 20 μm.

2.3. Devices fabrication

The PAA solutions were first diluted to solid contents (w/w) of 6% by using DMAc. Thus the diluted PAA solutions were cast on indium tin oxide (ITO) glasses by spin coating at 2000 rpm, followed by step-heating at 100 °C, 150 °C, 200 °C, and 250 °C under vacuum, each one for an hour to obtain the API thin films with thickness of 800 Å. The metal aluminum (Al) was deposited on the surface of the API films by using thermal evaporation under 5×10^{-6} Torr to form ITO/API/Al single layer LED devices.

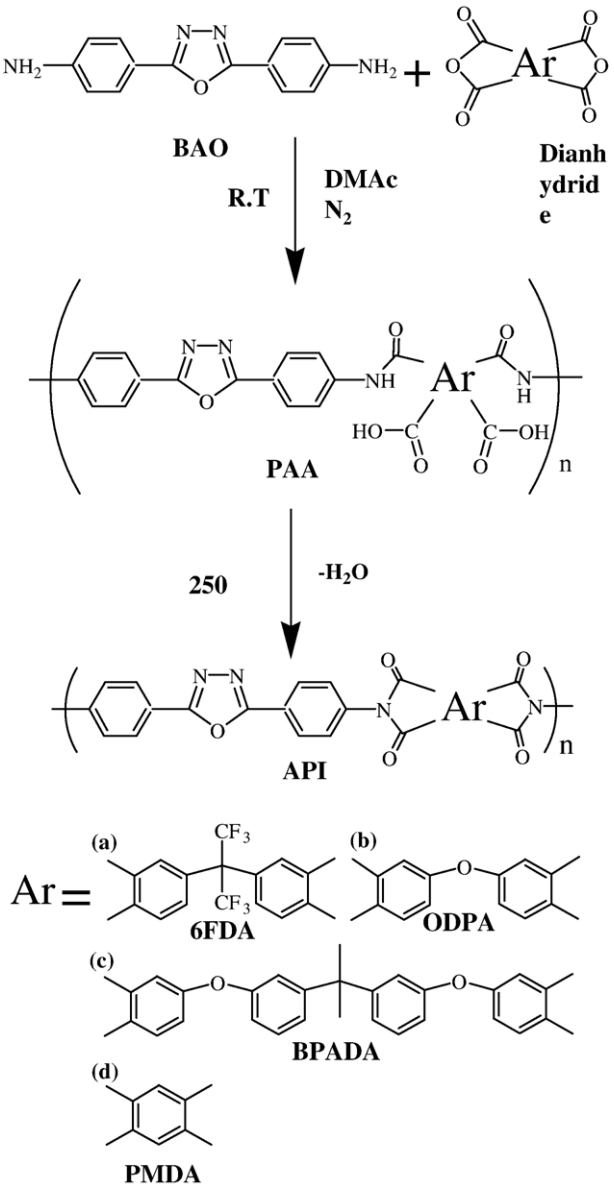

Scheme 1. The monomer structures and the synthetic route of the aromatic polyimides.

For the fabrication of the double layer LED device, the synthetic route of poly(*p*-phenylene vinylene) (PPV) precursor has been reported in our previous research paper in detail [37]. A 0.5% aqueous PPV precursor solution was mixed with 4.0% aqueous poly(vinylalcohol) (PVA, Mw = 72,000) solution by a weight ratio of 100/7. The PPV–PVA precursor was spin-coated on an ITO glass and then step-heated at 50 °C, 150 °C, 200 °C, and 300 °C, each one for an hour to obtain PPV–PVA thin film with thickness of 200 Å. PAA solution of 6% in solid content was then spin-coated on the PPV thin film and followed the same imidization process and the evaporation of the Al electrode as above.

2.4. Characterization

Thermal decomposition temperatures (T_ds) were measured by using TA Instruments TGA 2950 at a heating rate of 20 °C/min

Table 1
Inherent viscosity of the PAAs and thermal properties of the APIs

APIs	η_{inh} (dL/g) [a]	T_d [b] (°C)	T_g (°C)	CTE [c] (ppm/K)
BAO-PMDA	1.048	562	425	16.6
BAO-6FDA	0.993	540	350	49.9
BAO-ODPA	0.973	531	297	31.2
BAO-BPADA	0.401	514	257	86.1

[a] Measured in DMAc (C=0.5 g/dL) at 30 °C.
[b] 5 wt.% decomposition temperature measured under N_2.
[c] The CTE values are determined from 50 to 250 °C.

under nitrogen. The coefficients of linear thermal expansion (CTEs) were measured by using TA Instruments TMA 2940 at a heating rate of 10 °C/min, and the specimens were 12 mm long, 4 mm wide, and 20 μm thick. The glass transition temperatures (T_gs) were measured by using TA Instruments DMA 2980 Dynamic Mechanical Analyzer at a heating rate of 5 °C/min and a frequency of 1 Hz. Infrared (IR) spectra were measured by using Nicolet Protégé 460. Fluorescent spectra were obtained by using Shimadzu RF-5301 PC Spectrofluorophotometer with an excitation wavelength of 330 nm. The absorption spectra were obtained by using HP8453 UV–Vis spectrometer. The energy levels of the APIs were determined by UV–Vis absorption spectra and the data of cyclic voltammetry using CHI600A Electrochemical Analyzer. The cyclic voltammetry was carried out by using Pt counter electrode and an Ag/Ag^+ reference at the scan rate of 10 mv/s. The electrolyte was 0.1 M *tert*-$BuNClO_4$ in acetonitrile. Film thicknesses were measured by using Alpha Step Dektak ST surface profiler. The electroluminescence (EL) spectra were measured by using Jasco FR-770 spectrometer. The current–voltage characteristics of the LEDs were obtained by using Keithley 237 electrometer. The intensity–voltage characteristics were measured by using Keithley 237 electrometer with a photodiode detector of New Port power meter (Model 1815-C). The wide-angle X-ray diffraction (WAXD) patterns were obtained by MacScience MXP using Cu Kα radiation (50 kV, 200 mA, λ=1.54 Å) with a Monochromator.

3. Results and discussion

The structures of the APIs are determined by IR spectra (data not shown). The complete imidization was confirmed by the absence of characteristic peaks of PAA, such as C=O vibration band at 1670 cm^{-1} and O–H vibration band at about 3000 cm^{-1}, and the C=O vibration band of anhydride at 1850 cm^{-1}. Furthermore, the characteristic peaks of imide group at 1780 cm^{-1}, 1720 cm^{-1}, and 1380 cm^{-1} were found. The former two peaks are due to the asymmetric and the symmetric C=O stretching vibrations, and the last peak is associated with the C–N stretching [1].

The inherent viscosities of the resultant PAAs were measured by using Ubbelohde viscometer and the data were listed in Table 1. The inherent viscosities of the PAAs relate to the E_a of the dianhydrides. The tendency of the E_a of the dianhydrides is: PMDA > 6FDA > ODPA > BPADA [1,12]. The dianhydrides with higher E_a possess stronger electron-withdrawing ability in a nucleophilic substitution reaction of PAA formation, and assist in the formation of a higher molecular weight and viscosity.

The thermal properties of the APIs were listed in Table 1. All the APIs exhibit excellent thermal stabilities (T_d>500 °C). The APIs also show high T_g ranging from 257 to 425 °C. Especially in BAO-6FDA, the T_g value is 350 °C, which is higher than that of typical 6FDA-derived polyimides [38]. This may result from the oxadiazole-containing diamine, BAO, stiffening the main chain of the APIs [39,40]. The CTEs of the APIs were measured from 50 to 250 °C. BAO-PMDA has the lowest CTE, BAO-

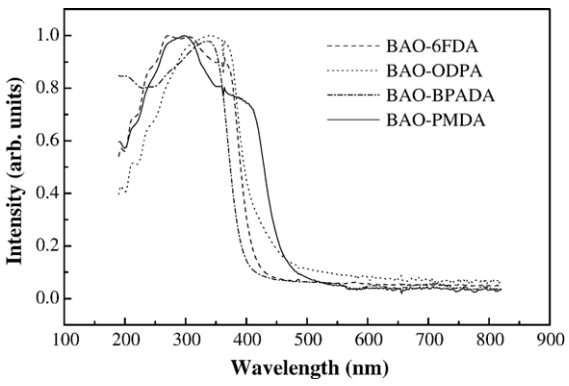

Fig. 1. Absorption spectra of the API films: BAO-6FDA, BAO-ODPA, BAO-BPADA and BAO-PMDA with 20 μm thickness.

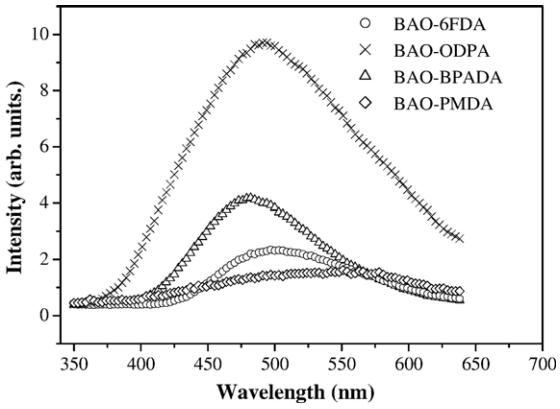

Fig. 2. Fluorescence spectra of the API films: BAO-6FDA, BAO-ODPA, BAO-BPADA and BAO-PMDA with 20 μm thickness.

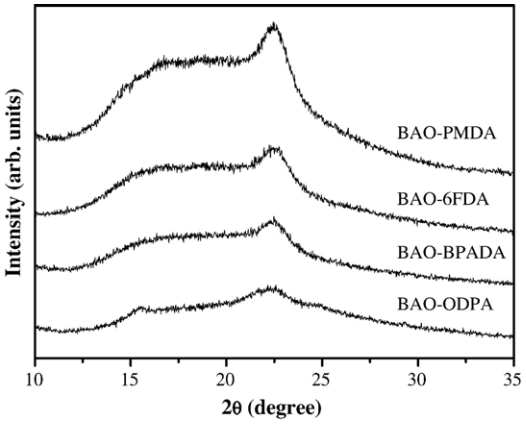

Fig. 3. WAXD patterns of the API films: BAO-6FDA, BAO-ODPA, BAO-BPADA and BAO-PMDA with 20 μm thickness.

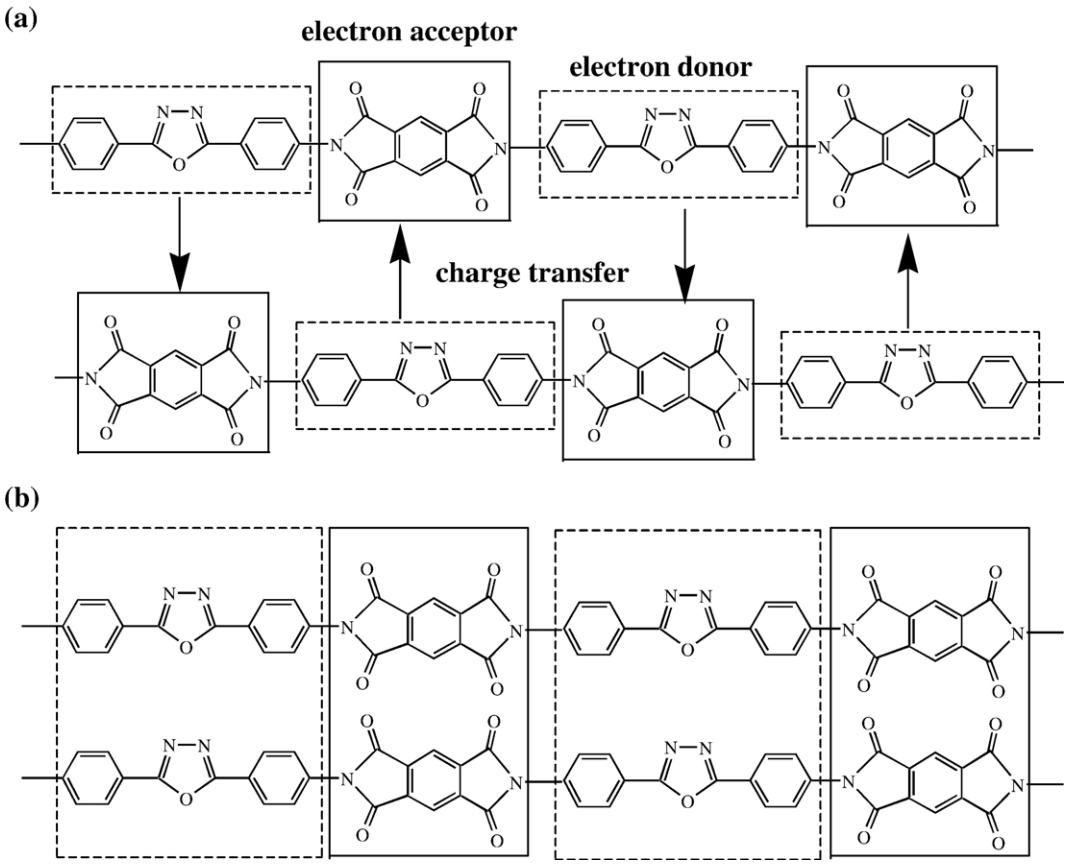

Fig. 4. The polyimide chain–chain interaction (a) CT interaction and (b) crystal.

ODPA and BAO-6FDA next, and BAO-BPADA is the highest. Numata et al. [41] pointed out that thermal expansion was an expansion of free volumes, and a low CTE resulted from small free volumes. BAO-PMDA with rod-like structure has dense molecular aggregation and exhibits small free volumes as well as low CTE, while BAO-BPADA contains bulky $-CH_3$ groups and two kink points of O groups in the dianhydride fragment. These disturb chain packing and increase the free volumes.

Fig. 1 shows the UV/Vis absorption spectra of the API films. BAO-PMDA and BAO-6FDA APIs have closely maxima absorption peaks at about 300 nm, and the shoulders are at 400 nm and 375 nm, respectively. However, BAO-ODPA and BAO-BPADA show a red-shift; both the maxima absorption peaks are at about 350 nm and on shoulders are found. The long-wavelength absorption in polyimides results from intermolecular CT interactions, and the enhancement of the red-shift with increasing intermolecular CT interactions [39]. This suggests that BAO-ODPA and BAO-BPADA may exhibit stronger intermolecular CT interactions than BAO-PMDA and BAO-6FDA APIs. This will be covered further on.

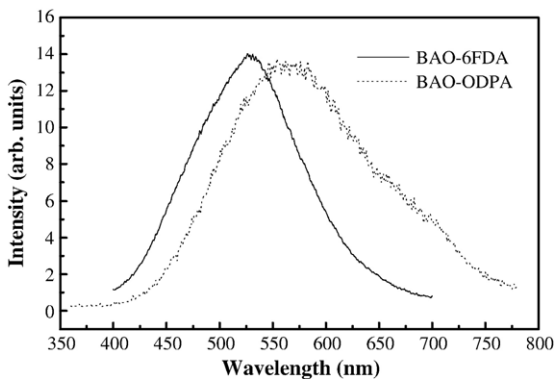

Fig. 5. Normalized electroluminescence spectra of the single layer API LED devices: ITO/BAO-6FDA/Al (—) and ITO/BAO-ODPA/Al (…).

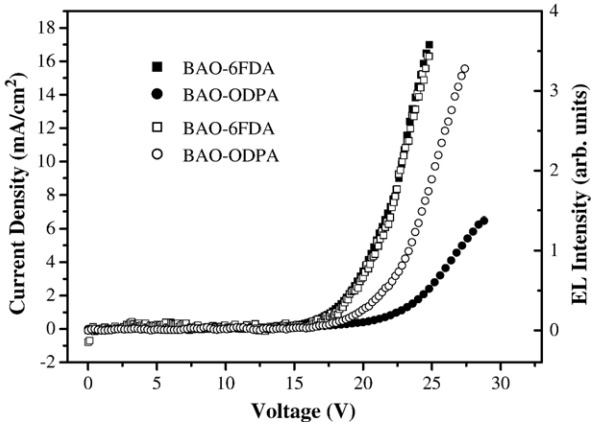

Fig. 6. Current density–voltage characteristics (closed mark) and EL intensity–voltage (open mark) for the single layer API LED devices: ITO/BAO-6FDA/Al (square) and ITO/BAO-ODPA/Al (circle).

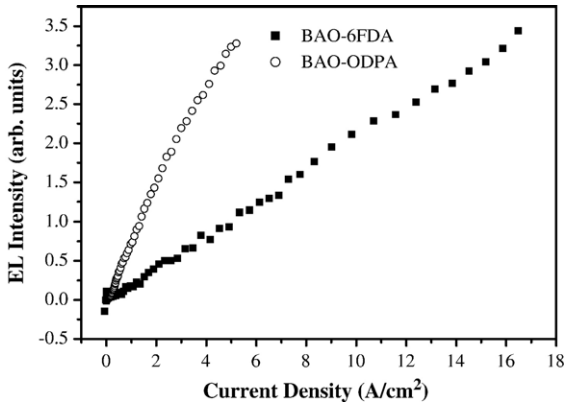

Fig. 7. EL efficiency for single layer API LED devices: ITO/BAO-6FDA/Al (■) and ITO/BAO-ODPA/Al (○).

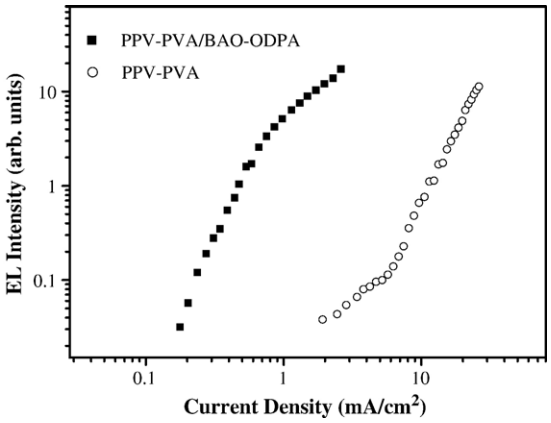

Fig. 9. EL efficiency of the LED devices: ITO/PPV–PVA/Al (○) and ITO/PPV/BAO-ODPA/Al (■).

Fig. 2 shows the fluorescent spectra of the API films. The APIs exhibit broad and structureless fluorescent properties [2–13]. For most of light-emitting polymers, an aggregation of molecular chains will assist an enhancement of fluorescence. In our case, BAO-PMDA, the densest molecular packing, shows the weakest fluorescent intensity, while BAO-ODPA is the strongest. This suggests that the CT fluorescence in polyimides not only relates to the molecular aggregation, but is also sensitive to the orientation of local structures. The WAXD was used to analyze the local ordering in the APIs. In Fig. 3, all the APIs have similar diffraction patterns and have crystalline structures. The tendency of the crystallinity is: BAO-PMDA > BAO-6FDA > BAO-BPADA > BAO-ODPA. This is just in revise order with the fluorescent intensity (Fig. 2).

Fig. 4 shows the chain–chain interaction of the intermolecular CT and the crystal along two neighboring chains [38]. In polyimides, the charge at HOMO and LUMO is localized at the electron-donating aminophenyl fragment and the electron-accepting imide fragment. This means that charge transfer can occur via the electron HOMO to LUMO transition, and the intermolecular CT is formed by the electron-donor (aminophenyl rings) and electron-acceptor (imide rings) belonging to adjacent molecular chains (Fig. 4a). However, when the molecular chains align in the form that the imide rings and the amine phenyl rings constitute separate layer (Fig. 4b), the intermolecular CT interaction would be reduced. Because exhibiting lower extent of the crystal, BAO-ODPA has more imide rings–aminophenyl rings face-to-face stacking, and shows the strongest fluorescent intensity than other APIs.

EL spectra of the BAO-ODPA and BAO-6FDA single layer LED devices are shown in Fig. 5. No EL property was found in BAO-PMDA LED device because of the intrinsic weakly fluorescence. BAO-BPADA LED device showed EL property, but too weak to be detected. It can be attributed to the large CTE. A polyimide film with large CTE will cause cracks and delamination during the thermal imidization or device operation, so the reliability and the efficiency of the devices will be reduced [1]. As shown in Fig. 5, the EL spectra of the APIs are similar to their fluorescent spectra (Fig. 2) indicating that the EL and the fluorescence may proceed the same radiative excited states in the APIs [42].

Fig. 6 shows the curves of current–voltage (I–V) and EL intensity–voltage (EI–V) of the single layer BAO-6FDA and BAO-ODPA LED devices. The current and emission intensity increases with increasing voltage, and both LED devices show

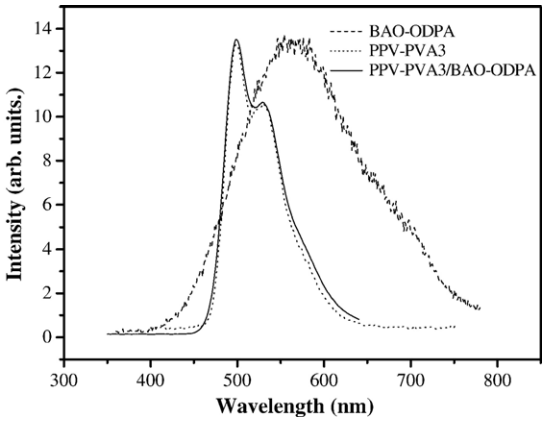

Fig. 8. Normalized electroluminescence spectra of the LED devices: ITO/BAO-ODPA/Al (---), ITO/PPV–PVA/Al (...) and ITO/PPV–PVA/BAO-ODPA/Al (—).

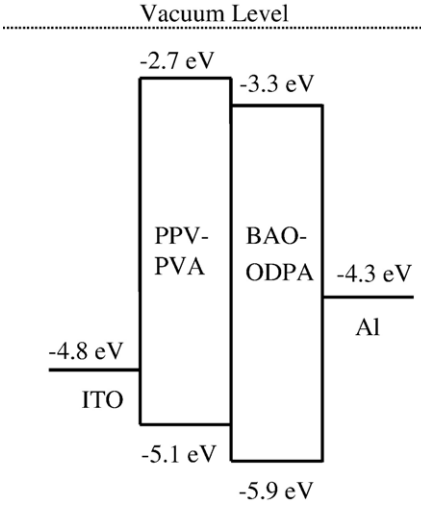

Fig. 10. Band diagram of ITO/PPV–PVA/BAO-ODPA/Al LED device.

the diode characteristic. From the EI–V curves, the threshold voltage (V_{th}) of BAO-6FDA and BAO-ODPA are 18 V and 22 V, respectively. The EL efficiency can be evaluated from the slope of the EL intensity versus current density. As seen in Fig. 7, the BAO-ODPA LED has a higher EL efficiency than the BAO-6FDA LED although the former has a higher V_{th}. It may suggest that the dianhydride structure has certain effects on the EL characteristics, and further investigation is underway.

As shown in Fig. 8, the EL spectrum of the double layer LED, ITO/PPV–PVA/BAO-ODPA/Al, is very similar to that of the single layer PPV–PVA device indicating that PPV acts as the emitting layer in the double layer device. The turn-on electric field of the double layer device is about 2.5×10^6 V/cm, and the operating voltage is higher than that of the single layer device (1.6×10^6 V/cm) due to the significant resistive voltage drop across the BAO-ODPA layer. Similar phenomena have been reported in other systems [43]. The EL efficiencies are shown in Fig. 9 (both axes are plotted in logarithmic scale). It shows that the double layer device incorporating BAO-ODPA has a higher EL efficiency than single layer PPV–PVA device; the EL efficiency of PPV–PVA light-emitting layer is improved by two orders of magnitude.

The energy band diagram of the double layer LED device is shown in Fig. 10. The energy barrier for electron injection decreases from 1.6 eV (in the single layer device) to 1.0 eV (in the double layer device). Moreover, the HOMO of BAO-ODPA (5.9 eV) is larger than that of PPV–PVA (5.1 eV). This means that BAO-ODPA provides both electron transport and hole blocking effect. BAO-ODPA has high HOMO and LUMO, so electron injection from the cathode is enhanced. The probability of radiative recombination in the light-emitting layer PPV–PVA is increased and enhances the EL efficiency. In addition, the BAO-ODPA layer separates the recombination zone from the metal electrode so that the recombination at the metal/polymer interface is avoided.

4. Conclusions

A series of BAO-based APIs have been synthesized. The APIs exhibit obvious fluorescent behavior and the fluorescent intensity relates to the crystalline degree. It is suggested that high crystallinity decreases the population of the imide rings–aminophenyl rings face-to-face stacking, so the CT interactions and the fluorescent intensity would be reduced. The resultant APIs not only can be a light-emitting layer in single layer LED, but also can act as an electron transport and an electron/hole blocking layer in a double layer PPV–PVA-based LED. The incorporation of BAO-ODPA layer into the PPV–PVA LED improves the EL efficiency by two orders of magnitude.

Acknowledgments

The authors gratefully acknowledge the National Science Council of the Republic of China and the Lee and MTI center in NCTU for the financial support of this work under Grant NSC 89-2216-E-009-024 and the research on photonic devices and modules project respectively.

References

[1] M.K. Ghosh, K.L. Mittal, Polyimides: Fundamentals and Applications, Marcel Dekker, New York, 1997.
[2] E.D. Wachsman, C.W. Frank, Polymer 29 (1988) 1191.
[3] H. Luo, L. Dong, H. Tang, F. Teng, Macromol. Chem. Phys. 200 (1999) 629.
[4] H. Ghassemi, J.H. Zhu, J. Polym. Sci., B, Polym. Phys. 33 (1995) 1633.
[5] J.P. Lafamina, S.A. Kafafi, J. Phys. Chem. 97 (1993) 1455.
[6] M. Hasegawa, I. Mita, M. Kochi, R. Yokota, Polymer 32 (1991) 3225.
[7] L. Qinghua, Y. Takashi, H. Kazutuki, Y. Hiroshi, J. Polym. Sci., A, Polym. Chem. 36 (1998) 1329.
[8] H. Masatoshi, J. Ishii, Y. Shindo, J. Polym. Sci., B, Polym. Phys. 36 (1998) 827.
[9] L. Weijin, A.F. Marye, J. Phys. Chem., B 101 (1997) 11068.
[10] H. Masatoshi, J. Ishii, Y. Shindo, Macromolecules 32 (1999) 6111.
[11] C.S. Ha, H.D. Park, C.W. Frank, Chem. Mater. 12 (2000) 839.
[12] M. Hasegawa, K. Horie, Prog. Polym. Sci. 26 (2001) 259.
[13] J.W. Yu, C.S.P. Sung, Macromolecules 30 (1997) 1845.
[14] R. Jakubiak, C.J. Collison, W.C. Wan, J. Phys. Chem., A 103 (1999) 2394.
[15] S. Setayesh, A.C. Grimsdale, T.F. Weil, J. Am. Chem. Soc. 123 (2001) 946.
[16] R.D. Scurlock, B.J. Wang, P.R. Ogilby, J. Am. Chem. Soc. 117 (1995) 10194.
[17] T. Zyung, J. Kim, Appl. Phys. Lett. 67 (1995) 3420.
[18] Y. Kim, J.G. Lee, D.K. Choi, Y.Y. Jung, B. Park, Synth. Met. 91 (1997) 329.
[19] Y.F. Wang, T.M. Chen, K. Okada, M. Uekawa, T. Nakaya, M. Kitamura, H. Inoue, J. Polym. Sci., A, Polym. Chem. 38 (2000) 2032.
[20] Y. Kim, J.G. Lee, K.J. Han, H.K. Hwang, Thin Solid Films 363 (2000) 263.
[21] J.G. Lee, S. Kim, D.K. Choi, Y. Kim, K. Kim, Phys. Soc. 35 (1999) S604.
[22] H.O. Ha, W.J. Cho, C.S. Ha, Mol. Cryst. Liq. Cryst. 349 (2000) 443.
[23] J.G. Lee, Y. Kim, S.H. Jang, S.N. Kwon, Appl. Phys. Lett. 72 (1998) 1757.
[24] E.I. Maltsev, M.A. Brusentseva, V.A. Kolesnikov, Appl. Phys. Lett. 71 (1997) 3480.
[25] E.I. Maltsev, V.I. Berendyaev, M.A. Brusentseva, Polym. Int. 42 (1997) 404.
[26] W.Y. Ng, X. Gong, W.K. Chan, Chem. Mater. 11 (1999) 1165.
[27] A.P. Wu, T. Akagi, M. Jikei, M. Kakimoto, Thin Solid Films 273 (1996) 214.
[28] P. Posch, M. Thelakkat, H.W. Schmidt, Synth. Met. 102 (1999) 1110.
[29] I.K. Spiliopoulos, J.A. Mikroyannidis, Macromolecules 31 (1998) 515.
[30] S.M. Pyo, S.I. Kim, T.J. Shin, M. Ree, Polymer 40 (1998) 125.
[31] S.M. Pyo, S.I. Kim, T.J. Shin, Macromolecules 31 (1998) 4777.
[32] Y. Kim, J.G. Lee, D.K. Choi, Y.Y. Jung, Synth. Met. 91 (1997) 329.
[33] Y. Kim, W.J. Cho, C.S. Ha, Mol. Cryst. Liq. Cryst. 294 (1997) 329.
[34] T. Matsumoto, K. Nishimura, T. Kurosaki, Eur. Polym. J. 35 (1999) 1529.
[35] W. Lu, J.P. Gao, Z.Y. Wang, G.G. Sacripante, Macromolecules 32 (1999) 8880.
[36] E.I. Mal'tsev, M.A. Brusentseva, V.I. Berendyaev, Mendeleev Commun. 1 (1998) 31.
[37] W.P. Chang, W.T. Whang, Polymer 37 (1996) 3493.
[38] D. Wilson, P. Hergenrothe, H.D. Stenzenberger, Polyimides, Chapmam & Hall, London, 1990.
[39] M. Zheng, L. Ding, P.M. Lahti, F.E. Karasz, Macromolecules 34 (2001) 4124.
[40] X. Zhan, Y. Liu, X. Wu, S. Wang, D. Zhu, Macromolecules 35 (2002), 2529.
[41] S. Numata, K. Fujisaki, N. Kinjo, Polymer 28 (1987) 2282.
[42] Z. Peng, J. Zhang, Chem. Mater. 11 (1999) 1138.
[43] M.Y. Hwang, M.Y. Hua, Polymer 40 (1999) 3233.